

Fabrication of Composite Membrane Based on Silicotungstic Heteropolyacid Doped Polybenzimidazole for High Temperature PEMFC

Jin-Woo Lee¹, Sher Bahadar Khan^{2,*}, Kalsoom Akhtar³, Kwang-In Kim¹, Tae-Won Yoo¹, Kwang-Won Seo¹, Haksoo Han^{1,*}, Abdullah M. Asiri²

¹ Department of Chemical and Biomolecular Engineering, Yonsei University, 262 Seongsan-no, Seodaemun-gu, Seoul 120-749, South Korea.

² Center of Excellence for Advanced Materials Research and Chemistry Department, Faculty of Science, King Abdulaziz University, Jeddah 21589, P.O. Box 80203, Saudi Arabia

³ Division of Nano Sciences and Department of Chemistry, Ewha Womans University, Seoul 120-750, South Korea.

*E-mail: sbkhan@kau.sa.edu; hshan@yonsei.ac.kr

Received: 7 May 2012 / Accepted: 12 June 2012 / Published: 1 July 2012

Stable proton conducting composite membranes (CM1-CM3) based on polybenzimidazole (PBI) and various weight percent (35, 50 and 65 wt %) of inorganic heteropoly acids (IHA) were prepared by dissolving PBI in methanesulfonic acid and required amount of IHA was then added to PBI solution. IHA were prepared by acid-catalyzed condensation of various ratios of silicotungstic acid (TSA) (35, 50 and 65 wt %) and silica (TEOS) (65, 50 and 35 wt %) using sol-gel procedure. These materials were characterized morphologically, studied their intrinsic structures and intimate relation with proton conductivity. It was found that thermal properties and proton conductivity of the composite membrane are strongly dependent on the IHA which increased with increase of IHA content. The composite membrane containing 65 wt % of IHA showed highest thermal property and proton conductivity. Composite membrane containing 65 wt% of IHA displayed highest conductivity of 2.91×10^{-1} S/cm at 150 °C. Thus introduction of IHA into PBI matrix is an efficient route to improve thermal properties and proton conductivity of PBI.

Keywords: Polybenzimidazole, Inorganic heteropoly acid, Silicotungstic acid, Composite membrane, Electrolyte, Proton conductivity

1. INTRODUCTION

Fuel cells membranes are emerging from the horizon as an alternative energy source for the mobile and home stationary energy application and thus electrolytic membranes for fuel cell

applications has gained much attention [1,2]. Fuel cell has also gained great attention due to high energy demand, high energy conversion efficiency, eco-friendly nature, simple storage of liquid fuel and elevated cost of petroleum. There are various types of fuel cells but among them, proton exchange membrane fuel cells (PEMFC) are considered one of the preeminent fuel cells. In proton exchange membrane fuel cells, membrane is used as an electrolyte which act as proton transport and avert fuel crossover [3,4].

Commercially available Nafion[®] was regarded as best polymer electrolyte membrane for its high proton conductivity, chemical and physical stabilities in past for many years. However it has functional limitations in operating temperatures which not exceeding above 90 °C and also its ion conductivity is contingent on the existence of water. Moreover it has a comparative short lifetime if hydrogen containing traces of carbon monoxide is fed to the electrolyte because carbon monoxide is poison for the anode catalyst at low temperature circumstances [5]. Carbon monoxide always exist in hydrogen obtained by reforming process of hydrocarbons or methanol and elimination of small amount of carbon monoxide from the hydrogen is highly cost additive process in the cell operation. It is known that the resistance of platinum anode catalyst to the carbon monoxide poisoning needs higher operation temperature of fuel cell and thus less expensive stable membranes working at high operational temperatures more than 100 °C and low relative humidity is urgently required because the operation of membrane at temperature above 100 °C exhibits higher tolerance toward hydrogen impurities, better control with a simple system design and operation, higher efficiency and higher power density [6-8].

Thus fabrication of polymer electrolyte membrane fuel cells (PEMFCs) which can operate at high temperature is one of the great challenges for the scientific community because the operation at high temperature increases the kinetics of both electrodes and increase the tolerance of the Pt electrodes to carbon monoxide. The current research on fuel cell is based on purpose to craft a device working at high operational temperatures more than 100 °C and low relative humidity. Hence, great hard work have been devoted to the invention of alternative proton exchange membrane which not only can work at higher temperature but possess high proton conductivity and thermal stability [9-11].

For the development of high temperature operational polymer membrane, one of the new polymers among many studies that are in progress is polybenzimidazole (PBI). PBI is on the spotlight as the most suitable electrolyte membrane for high temperature PEMFC because of its excellent properties such as thermal stability, impact resistance, and chemical resistance. Phosphoric acid doped polybenzimidazoles have achieved more and more attention for their high ionic conductivity at higher temperature up to 200°C under anhydrous conditions, and excellent oxidative and thermal stability [12-18]. That is why PBI is considered as the most capable candidates for fuel cell due to its high performance and low cost properties. The doping level of phosphoric acid determines the proton conductivity of PBI. But higher phosphoric acid loading level has some drawbacks i.e, loss of the mechanical property as well as leaching out of unbound acid with the phosphoric acid doping level improvement. In order to solve the above mentioned problem, modification of the PBI matrix by addition of inorganic filler is required. These approaches have certainly improved the performance of the PBI. The introduction of inorganic proton donors into the polymer electrolyte matrix increases various properties of the polymer electrolyte such as proton conductivity, thermal stability etc, and therefore it gained a lot of attention due to their excellent performance in various aspects. In this

contribution silicotungstic hetero poly acid has been selected as inorganic filler for the enhancement of thermal properties and proton conductivity of PBI.

Silicotungstic heteropoly acid is an inorganic proton donor and has shown high stability and conductivity. It subsist in hydrate phases ($H_3SiW_{12}O_{40} \cdot nH_2O$) in the form of Keggin Unit which is a cluster of $[PM_{12}O_{40}]^{+3}$. These crystalline hydrated heteropoly acids have shown high proton conductivity, protect Pt anode catalyst from CO poisoning and positive effect on the electrochemical reduction of oxygen. Silicotungstic hetero poly acid increase reaction kinetics and increases the catalytic activity at higher temperatures for both electrodes. It has shown fast electro-kinetics and less CO poisoning between the electrode and electrolyte and shown hopeful effect on the electrochemical reduction of oxygen at the cathode site [19-21].

In this contribution, PBI has been synthesized by polymerization reaction of 3,3-diaminobenzidine and pyridine-2,5-dicarboxylic acid using PPA as a condensation reagent. The synthesized PBI was doped with various wt% of IHA and characterized by Fourier transform infrared spectroscopy whereas the morphologies were confirmed via X-ray diffraction and scanning electron microscopy. The composite membranes showed high thermal stability and excellent proton conductivity which were confirmed by TGA, DSC and impedance analyzer. Further by comparing with PBI, the composite membrane exhibited superior performance than PBI in terms of thermal stability and proton conductivity.

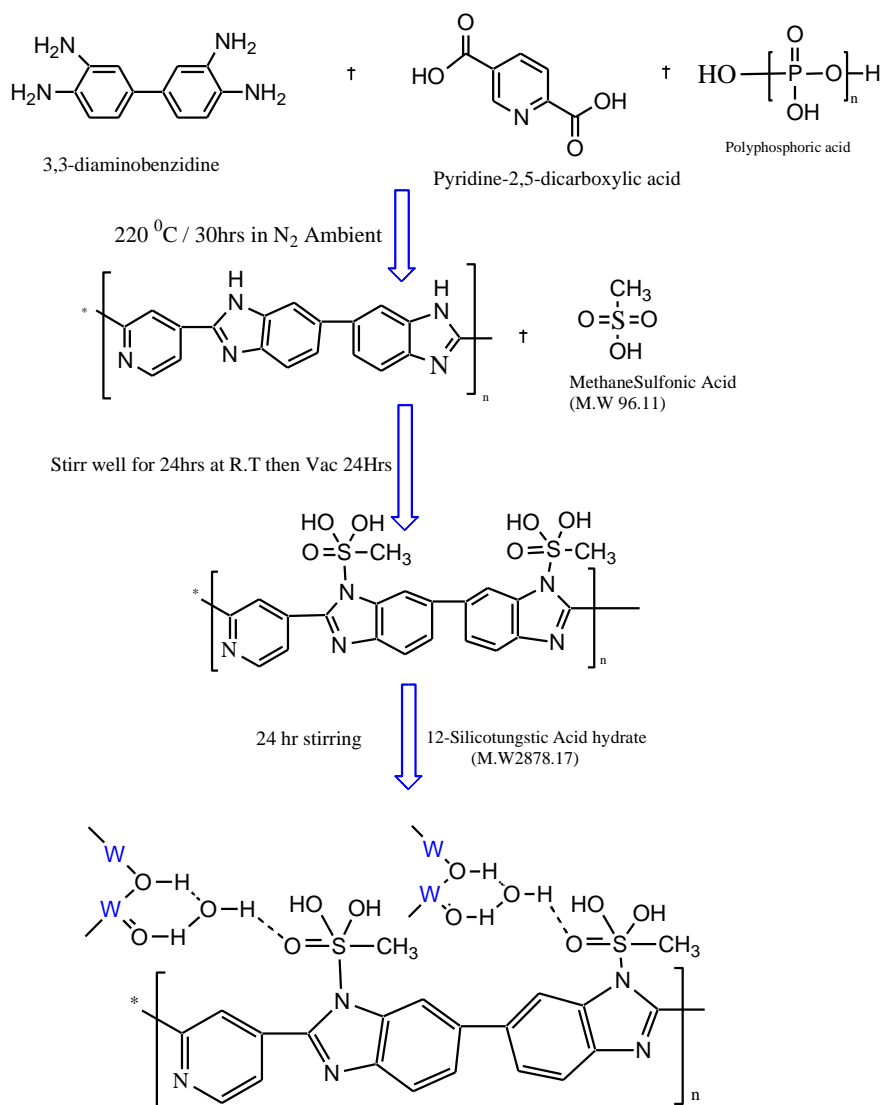
2. EXPERIMENTAL

2.1. Materials

The materials were prepared by using silicotungstic acid hydrate $H_4[SiW_{12}O_{40}] \cdot nH_2O$ and purity 99.99% tetraethoxyorthosilicate (TEOS) and silica (surface area $390 \pm 40 \text{ m}^2/\text{g}$) from Sigma Aldrich were used as received. All the chemicals and D.I water were of reagent grade and used without further purification.

2.1. Synthesis of PBI

PBI has been synthesized by polymerization reaction of 3,3-diaminobenzidine and pyridine-2,5-dicarboxylic acid using PPA as a condensation reagent. Both 3,3-diaminobenzidine and pyridine-2,5-dicarboxylic acid were added into a 250ml three-necked round-bottom flask containing PPA equipped with a mechanical stirrer, thermometer, nitrogen inlet and a reflux condenser. The mixture was stirred at room temperature using mechanical stirrer for a certain time until it became homogenous. Then the reaction was heated to $220 \text{ }^\circ\text{C}$ and purged with a slow stream of nitrogen. After 30 hours, the mixture was poured into de-ionized water and neutralized by KOH (1mol/L) and washed by boiling water for several times to eliminate exceeded phosphoric acid. After filtration, polymer was dried in a vacuum oven at $120 \text{ }^\circ\text{C}$ for 24 hours. The whole procedure is schematically sketched in scheme 1.



Scheme 1. Synthetic scheme of PBI and composites.

2.2. Preparation of inorganic heteropoly acid (IHA) materials

Hetero poly acid matrices (IHA-1, IHA-2, IHA-3) composed of TSA and SiO_2 with 35:65 (IHA-1), 50:50 (IHA-2), 65:35 (IHA-3) were prepared by acid-catalyzed condensation of various ratios of TSA and TEOS using sol-gel procedure. Typically, the required amount of TEOS was well dispersed in ethanol. Then 8 wt% of HNO_3 was added to the mixture followed by addition of TSA with continuous stirring. The resulting solution was titrated with 1N NaOH solution and continued the stirring for three hours until suspension is obtained. The resulting product was dried at 100°C for 24 hours. The dried product was grinded and fine powder was obtained. The synthesis of IHA has been given in scheme 1.

2.3. Preparation of composites membranes

The composites membranes based on various inorganic heteropolyacid material (IHA) and 2,5-polybenzimidazole (PBI) were prepared by dissolving PBI in methane-sulfonic acid and required amount of IHA (35, 50, 65 wt %) was then added to PBI solution (65, 50, 35 wt %). The resulting solution was magnetically stirred for 24 hours and then cast on a glass by spine coating. Films of 50~80 μm thickness were obtained after drying. The prepared membrane was soaked in 95 wt% phosphoric acid solution at room temperature for 72 hours before impedance measurement. The thicknesses of the acid treated membranes were measured prior to equip with impedance analyzer and performed a series of electrical characterization test. Composite membranes containing 35, 50 and 65 wt % of IHA was noted as CM-1, CM-2, CM-3, respectively (Table 1). Synthesis of composite membranes is shown in scheme 1.

Table 1. Heteropoly acid ratio of membranes.

Sample	wt% (IHA)	wt% (TSA)	wt% (Si)	wt% (PBI)	Mechanical stability	Wet in H_3PO_4 in 72 Hr
CM-1	35	16.5	18.5	65	Stable	Wet
CM-2	50	22.5	27.5	50	Stable	Wet
CM-3	65	28.5	36.5	35	Stable	Wet

2.4. Doping level

Before measurements of proton conductivity of PBI and composite membranes containing IHA powders, all the membranes were dipped in 83.5 wt% phosphoric acid solution for 72 hrs and the doping level was measured by calculating the weight difference before and after dipping in phosphoric acid solution. The acid sorption behavior of the PBI and composites are shown in Table 2. PBI showed lower doping level while the degree of sorption of acid (doping level) increased with increase of wt % of IHA in composites. The high doping level of composites might be due to IHA, to which high amount of phosphoric acid will connect rather than that of PBI. The doping amount of phosphoric acid is mainly responsible for proton conductivity of the membrane. Thus, after doping with phosphoric acid composites membrane could have better proton conductivity than the PBI membrane.

Table 2. Doping density of phosphoric acid (H₃PO₄) in membranes.

Sample	Area	Thickness (μm)	Amount of doped H ₃ PO ₄ (g)	Amount of phosphoric acid per specific volume (g/μm ³)
PBI	1 cm x 1 cm	86 μm	0.0149 g	1.73E-12
CM-1	1 cm x 1 cm	110 μm	0.0407 g	3.70E-12
CM-2	1 cm x 1 cm	120 μm	0.0472 g	3.93E-12
CM-3	1 cm x 1 cm	122 μm	0.0488 g	4.00E-12

2.5. Characterization of IHA, PBI and composite materials

2.5.1. FT-IR Analysis

FT-IR analysis was done in the range of 500 to 4000 cm⁻¹ using FTIR spectrophotometer (Varian resolution Pro).

2.5.2. Thermal Gravimetric Analysis (TGA)

Thermal gravimetric analyses were performed in the temperature range of 30 to 600 °C using Q50 (TA instrument) in nitrogen atmosphere with the scanning rate of 20 °C /min.

2.5.3. Differential Scanning Calorimetric analysis (DSC)

Differential scanning calorimetric analysis were done in the temperature range of 30 to 500 °C using Q10 (TA instrument) in nitrogen atmosphere with scanning rate of 10 °C /min.

2.5.4. X-ray Diffraction Analysis (XRD)

X-ray diffraction analysis were performed with a Philips X-Pert diffractometer using a Cu-Kα radiation (λ=1.5405Å) and operating at 40kV and 30mA with 2 range of 5-90°. The X-ray diffraction patterns were collected with a scan rate of 0.5°/min.

2.5.5. Scanning Electron microscopic Analysis (SEM)

The morphology of PBI and the composite membranes were studied by scanning electron microscope, JEOL (JSM840A).

2.5.6. Impedance Analysis measurement

Proton conductivity was measured using electrochemical impedance spectroscopy technique. The resistances of membranes were measured by Auto Lab Impedance Analyzer and proton conductivity cell. The proton conductivity (σ) of all membranes after recording up to 150 °C was calculated by the following equation:

$$\sigma = \frac{d}{L_S W_S R}$$

Where d , L_S , W_S and R are the distance of the electrodes, film thickness, film width and the resistance of the membrane respectively [22,23].

3. RESULTS AND DISCUSSION

PBI has both donor and acceptor bonding sites and is thus capable of specific ion interaction. In the presence of acid or bases, PBI poly-cations will form and thus result in salt formation. The polymer electrolytes as a proton donor were functionally activated with IHA to increase the proton conductivity in the membrane. Also silicotungstic acids $[[H_4SiW_{12}O_{40}].H_2O]$ are known as strong Bronsted acid as solid electrolytes which can preferably dissociate four protons in solution. The route for the formation of such materials is sol-gel technique which comprises of hydrolysis and condensation of precursor molecules (alkoxides) under mild conditions. Silicotungstic acid exhibits a good solubility in simple alcohol-water solvents and also keeps good stability when it is adsorbed in tetraethoxyorthosilicate (TEOS) during the sol-gel process. Silicotungstic acid (TSA) obeys Onsager–Fuoss theory for strong electrolyte and behaves as acid in water or mixed water alcohol solvents. That means silicotungstic acid acts as tungsten precursor and as acid catalyst for the hydrolysis of silicon alkoxides [19,20].

3.1. Structural characterization

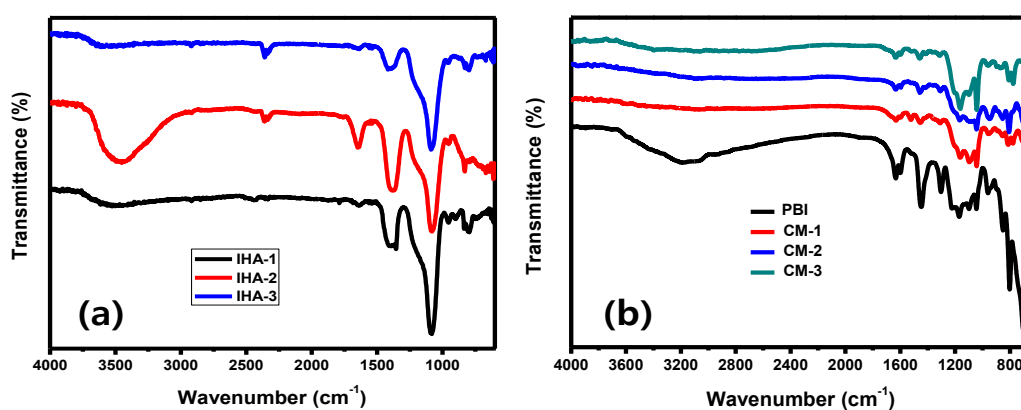


Figure 1. FT-IR spectra of IHA-1, IHA-2 and IHA-3 and CM-1, CM-2, CM-3.

IHA were structurally characterized by FTIR and the data is shown in Fig. 1(a). In FT-IR spectrums of IHA, tungsten oxide and silinol group showed absorption bands at 790, 835, 900, 955, 1013 cm^{-1} which are due to W-O, W-O-W bonds, Si-O and Si-O-Si bonds [19]. The peak at 1640 and 3430 cm^{-1} are responsible for bending and stretching vibration of H_2O which normally mesoporous materials absorb from the environment. FTIR spectrum of PBI (Fig. 1(b)) exhibited peaks at 3300 cm^{-1} which is responsible for N-H stretching. It also showed at peak at 1660 cm^{-1} which is due to C=C bond stretching. Similarly it also showed bending and stretching band for C-C bond (1100 cm^{-1}), C-N stretching band (1350 cm^{-1}) and C=N band (1610 cm^{-1}). All the FTIR peaks of both PBI and IHA were detected in CM-1, CM-2 and CM-3 which confirm that the composites membranes were successfully synthesized [24,25].

3.2. Morphological characterization

The morphological structures of IHA were analyzed by wide angle X-ray diffraction (XRD) which is shown in Fig. 2. The general aspect of this XRD patterns, in particular the presence of strong diffraction halo and absence of sharp crystalline peaks indicate the presence of amorphous phase only and show the absence of crystalline phase or crystalline-amorphous phase formation.

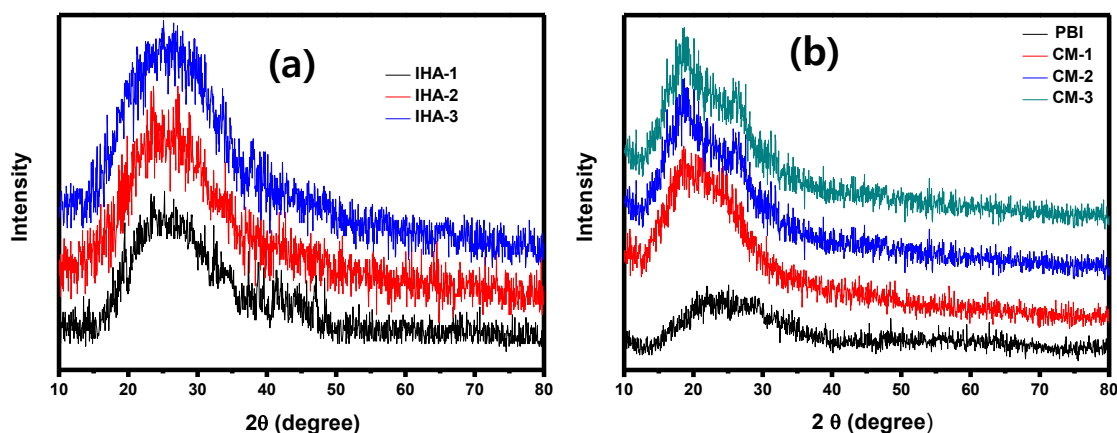


Figure 2. Typical XRD spectrum of (a) IHA-1, IHA-2, IHA-3 and (b) PBI, CM-1, CM-2, and CM-3.

Thus XRD pattern of IHA-1, IHA-2 and IHA-3 did not show any crystalline or semi-crystalline peaks which indicate that IHA-1, IHA-2 and IHA-3 are amorphous materials. IHA-1, IHA-2 and IHA-3 exhibited very broad peak at $2\theta = 26^\circ$ ($d = 1.75\text{\AA}$) which is a characteristic peak of amorphous materials [26]. XRD spectrum of PBI membrane exhibited a broad halo in the area of 2θ from 15° to 40° without any crystalline peaks which confirm that PBI membrane is amorphous in nature. This means PBI and composite membranes have amorphous structure. The XRD spectrum of composite does not show any characteristic peaks of crystalline structure which clearly shows that the IHA were uniformly distributed in the PBI membrane without any agglomeration and aggregation. Other several researchers have also found the same broad amorphous peak in the same region [27,28].

Fig. 3 shows SEM images of PBI and composite membranes (CM-1, CM-2 and CM-3). SEM image of PBI shows aggregation of particles while in case of composites, IHA particles are well dispersed in PBI matrix. The SEM images of the composites show dense structure with agglomeration of particles.

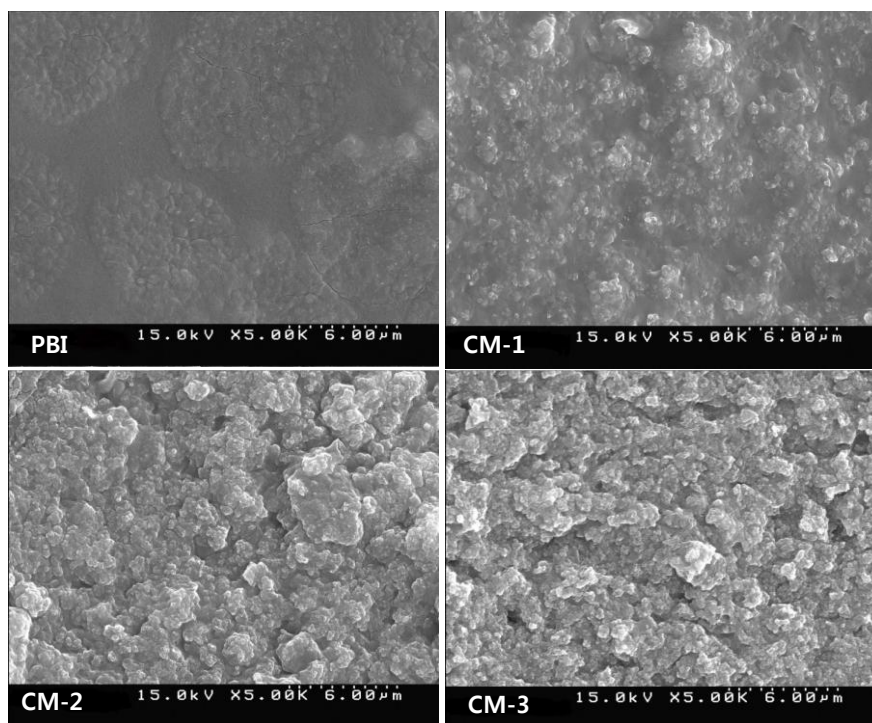


Figure 3. Scanning electron images of PBI, CM-1, CM-2, and CM-3.

3.3. Thermal Properties

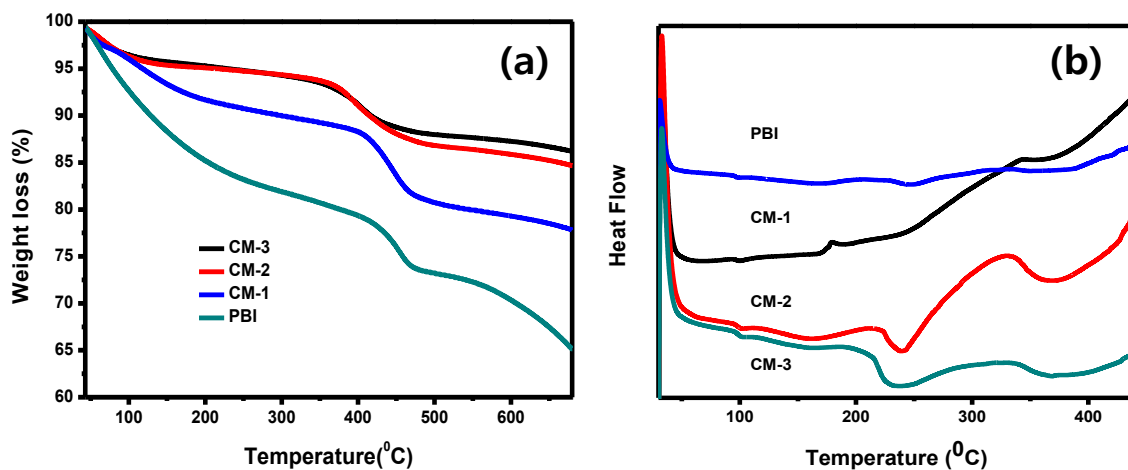


Figure 4. (a) TGA and (b) DSC curves of PBI, CM-1, CM-2, and CM-3.

In an effort to study the effect of IHA on the thermal stability of PBI membrane, we have examined TGA and DSC. TGA and DSC for both PBI and composite membranes were measured under nitrogen atmosphere and patterns are presented in Fig. 4(a) and 4(b), respectively. TGA of PBI shows first weight loss at temperature 100 ~ 250 °C which is around 20% weight loss, the second step start from 411 to 480 °C which is around 7% weight loss. The first step of degradation involves evaporation of physically absorbed solvent and residual monomers while the second weight loss is due to the decomposition of the main polymer chain. In case of composites, the weight lost percent decreases as the IHA weight percent increases. In composite containing 35 wt% of TSA, the first weight loss occurred in the temperature range of 100 ~ 200 °C is account to around 9% weight loss, the second step from 400 to 485 °C is account to around 7% weight loss. Composite containing 50 wt% of IHA showed the first weight loss in the temperature range of 50 ~ 140 °C is accounted to around 5% weight loss, the second step from 350 to 485 °C is accounted to around 7% weight loss. Composite containing 65 wt% of IHA showed the first weight loss in the temperature range of 50 ~ 130 °C is accounted to around 5% weight loss, the second step from 350 to 485 °C is accounted to around 7% weight loss. When we compared the TGA curves of all the composites with PBI, all composite membranes show less thermal degradation than that of pure PBI. This confirms that thermal stability of the composite mainly depends on the addition of IHA. Table 3 summarizes 5% and 10% weight loss decomposition temperatures of PBI and composites, defined as $T_{d5\%}$ and $T_{d10\%}$ respectively [24-30].

The DSC data of PBI and composites are depicted in Fig. 4(b). PBI exhibits a glass transition temperature (T_g) at 340 °C (Table 3). With the addition of IHA, the glass transition temperatures of composites obviously increased and showed the T_g at 346 °C which is 6 °C higher than that of PBI. This is because of the strong interaction between the PBI and IHA which restricts the segmental motion of PBI molecular chains [24-30].

Table 3. TGA and DSC results of PBI, CM-1, CM-2 and CM-3.

Samples	5% wt loss	10% wt loss	TG
PBI	78.58	128.82	340.45
CM-1	229.26	416.74	346.23
CM-2	214.1	414.57	346.39
CM-3	118.2	299.91	346.33

3.4. Proton conductivity

To evaluate the fuel cell performance of PBI and composite membranes (CM-1, CM-2 and CM-3), proton conductivities of all the membranes were studied which is the most important property

of the polymer membrane and the charge density of the fuel cell depends on the proton conductivity. Therefore polymers with high proton conductivity are highly desired. The proton conductivity of the phosphoric acid doped PBI and phosphoric acid doped composite membranes were measured at 150 °C temperature and the graph is shown in Fig. 5. PBI and composite membranes gives initial proton conductivity of $2.86\sim 3.88 \times 10^{-1}$ S/cm at 150 °C. CM-3 exhibited highest proton conductivity (2.93×10^{-1} S/cm) as compared to all other membranes even higher than that of reported by P. Staiti et al for silicotungstic acid with polybenzimidazole which was 2.28×10^{-1} S/cm at 150 °C [31-33]. This clearly indicates that mesoporous silica with tungstic acid Keggin network structure improves the conductivity behavior of the membranes because of high absorption level of phosphoric acid and thus creating an alley for proton transfer.

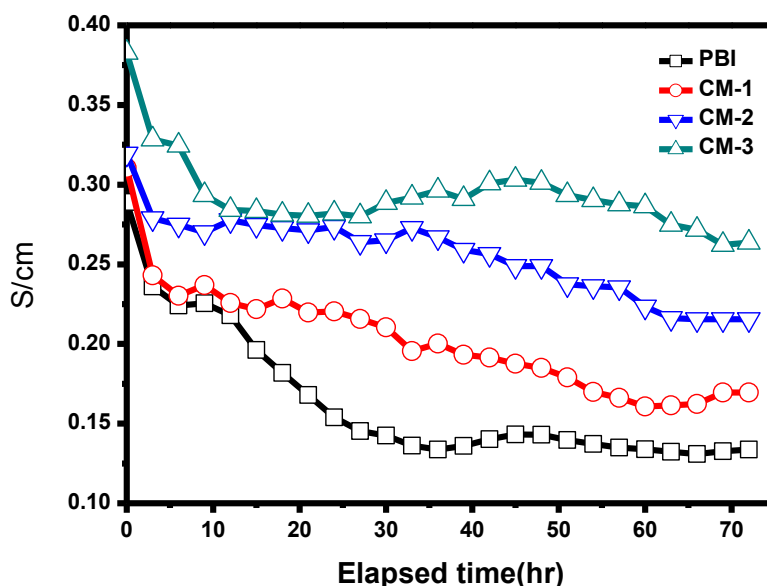


Figure 5. Proton conductivities of phosphoric acid doped PBI, CM-1, CM-2, and CM-3.

PBI and composite membranes showed proton conductivity in the order of $CM-3 > CM-2 > CM-1 > PBI$ with proton conductivity values $2.93 \times 10^{-1} > 2.56 \times 10^{-1} > 2.02 \times 10^{-1} > 1.64 \times 10^{-1}$ S/cm.

All the composites showed much higher proton conductivity than Nafion117[®] having proton conductivity of 0.187 Scm^{-1} at 90 °C and 100% humidity [34]. Trapped water inside Nafion117[®] structure play important role towards its proton conductivity for the most part and this limit the Nafion117[®] to work at the temperature above 100 °C. Reverse is the case considering composites, its proton conductivity increases with the increasing temperature. When the temperature was increased from 40 °C to 150 °C for composites the proton conductivity was increased which narrowed its margin compared with the Nafion117[®] operating at the limited operating temperature (below 100 °C). In another words, working at high temperature composite membranes can possibly be a substitute for Nafion[®] in PEMFC [34].

The proton transport in phosphoric acid doped composite membranes is determined by quantity of IHA, phosphoric acid connected to composite membranes by hydrogen bonding and free acids

called hydronium. Considering these two different phosphoric acids, the proton transport inside the polymer followed two principles. One, the rapid proton exchange between the bonded acids or the bonded acids and the composite by Grotthuss mechanism and the second one is based on the self-diffusion of free phosphoric acids by Vehicle mechanism [35]. Temperature increase stimulated both the ways involved in proton transfer and the structural reorganization required for good proton conductivity. As compared to PBI, the composites exhibited higher proton conductivity at the same temperatures, due to the IHA density contained by the composite which gives the PBI a higher phosphoric acid doping level. Composites showed high proton conductivity as both the bonded acids and the free acids are improved, verifying much more proton carrying ability of composites [35].

4. CONCLUSION

PBI and their composites membrane were synthesized and applied for high temperature proton exchange membrane fuel cell. PBI was synthesized by polymerization reaction of 3,3-diaminobenzidine and pyridine-2,5-dicarboxylic acid while their composite were synthesized by composition with various wt% of IHA. PBI and composites membranes were structurally and morphologically characterized by FTIR, XRD and SEM. PBI and composites membranes showed high thermal and conductivity properties. According to the TGA and DSC analysis, the PBI and composites membrane can be operated up to 200 °C. Among all membranes, CM-3 showed higher proton conductivity as $2.93 \times 10^{-1} \text{ Scm}^{-1}$ at 150 °C which may be due to high phosphoric acid doping level which can be owed to the large contents of IHA contained by the PBI. From high proton conductivity performance of composite membranes, it is concluded that the synthesized composite membranes can be used as promising proton exchange membranes for high temperature proton exchange membrane fuel cell.

ACKNOWLEDGEMENTS

This work was supported by the National Research Foundation of Korea Grant founded by the Korean Government (MEST) (NRF-2009-C1AAA001-0092926) and the National Research Foundation (NRF) of Korea Grant founded by the Korean Government (MEST) (No. 2011-0016750).

References

1. F. Seland, T. Berning, R. Tunold, *J. Power Sources*, 160 (2006) 27-36.
2. L. Xiao, H. Zhang, B. C. Benicewicz, *Chem. Mater.* 17 (2005) 5328-5333.
3. A. Carollo, E. Quartarone, C. Tomasi, P.P. Righetti, *J. Power Sources*, 160 (2006) 175-180.
4. L. Xiao, H. Zhang, L. S. Ramanathan, C. Benicewicz, *Fuel Cells*, 5 (2005) 287-295.
5. T. J. Schmidt, H. A. Gasteiger, R. J. Behm, *J. New Mat. Electrochem. Systems*, 2 (1999) 27-32.
6. Q. Li, R. He, J. O. Jensen, N. J. Bjerrum, *Chem. Mater.* 15 (2003) 4896-4915.
7. J. Zhang, Z. Xie, J. Zhang, Y. Tang, C. Song, T. Navessin, *J. Power Sources*, 160 (2006) 872-891.
8. W. H. J. Hogarth, J. C. D. Costa, G. Q. Lu, *J. Power Sources*, 142 (2005) 223-237.
9. O. Nakamura, I. Ogino, T. Kodama, *Solid state ionics*, 3 (1981) 347-351.

10. P. Krishnan, J. S. Park, C. S. Kim, *J. Power Sources*, 159 (2006) 817-823.
11. M. Helen, B. Viswanathan, *J. Membrane Science*, 292 (2007) 98-105.
12. Q. Li, R. He, J. O. Jensen, N. J. Bjerrum, *Fuel Cells*, 4 (2004) 147-159.
13. J. Lobato, P. Canizares, M. A. Rodrigo, J. J. Linares, G. Manjavacas, *J. Membr. Sci.* 280 (2006) 351-362.
14. Q. Li, H. A. Hjuler, N. J. Bjerrum, *J. Appl Electrochem.* 31 (2001) 773-779.
15. T. Kim, T. Lim, J. Lee, *J. Power Sources*, 172 (2007) 172-179.
16. S. R. Samms, S. Wasmus, R. F. Savinell, *J. Electrochem. Soc.* 143 (1996) 1225-1232.
17. D. Weng, J.S. Wainright, U. Landau, R.F. Savinell, *J. Electrochem. Soc.* 143 (1996) 1260-1263.
18. K. D. Kreuer, *J. Member. Sci.* 185 (2001) 29-39.
19. M. Klisch, *J. Sol-Gel sci. technol.* 12 (1998) 21-33.
20. A. Verma, K. Scott, *J. Solid State Electrochem.* 14 (2008) 213-219.
21. J. Lobato, P. Canizares, M. A. Rodrigo, J. J. Linares, J. A. Aguilar, *J. Membr. Sci.* 306 (2007) 47-55.
22. M. A. Hickner, H. Ghassemi, Y. S. Kim, B. R. Einsla, J. E. McGrath, *Chem. Review*, 104 (2004) 4578-4611.
23. M. L. Hill, Y. S. Kim, B. R. Einsla, J. E. McGrath, *J. Membr. Sci.* 283 (2006) 102-108.
24. S. B. Khan, M. M. Rahman, E. S. Jang, K. Akhtar, H. Han, *Talanta*, 84 (2011) 1005-1010.
25. S. B. Khan, J. C. Seo, E. S. Jang, J. S. Choi, S. H. Choi, H. Han, *Mem. J.* 19 (2009) 341-347.
26. S. Choi, S. Lee, J. Jeon, J. An, S. B. Khan, S. Lee, J. Seo, H. Han, *J. Appl. Polym. Sci.* 117 (2010) 2937-2945.
27. S. B. Khan, J. Seo, E. S. Jang, K. Akhtar, K. I. Kim, H. Han, *Macromol. Res.* 19 (2011) 876-882.
28. E. S. Jang, S. B. Khan, J. Seo, K. Akhtar, J. Choi, K. I. Kim, H. Han, *Macromol. Res.* 19 (2011) 1006-1013.
29. E. S. Jang, S. B. Khan, J. Seo, Y. H. Nam, W. J. Choi, K. Akhtar, H. Han, *Prog. Org. Coat.* 71 (2011) 36-42.
30. E. S. Jang, S. B. Khan, J. Choi, J. Seo, H. Han, *J. Chem. Soc. Pak.* 33 (2011) 549-554.
31. P. Staiti, S. Hocevar, N. Giordano, *Int. J. Hydrogen Energy*, 22 (1997) 809-814.
32. P. Staiti, A.S. Arico, V. Antonucci, S. Hocevar, *J. Power Sources*, 70 (1998) 91-101.
33. P. Staiti, *J. New Mat. Electrochem. Systems*, 4 (2001) 181-186.
34. J. Seo, W. Jang, S. Lee, H. Han, *Polym. Degrad. Stabil.* 93 (2008) 298-304.
35. C. Liu, S. B. Khan, M. Lee, K. I. Kim, K. Akhtar, H. Han, A. M. Asiri, *Macromol. Res.* (2012)...in press.